

Jones matrix treatment for optical Fourier processors with structured polarization

Ignacio Moreno,^{1,*} Claudio Iemmi,² Juan Campos,³ and Maria J. Yzuel³

¹Dept. Ciencia de Materiales, Óptica y Tecnología Electrónica. Universidad Miguel Hernández, 03202 Elche, Spain

²Departamento de Física. Universidad de Buenos Aires, Argentina

³Departamento de Física, Universitat Autònoma de Barcelona, 08193 Bellaterra, Spain

*i.moreno@umh.es

Abstract. We present a Jones matrix method useful to analyze coherent optical Fourier processors employing structured polarization. The proposed method is a generalization of the standard classical optical Fourier transform processor, but considering vectorial spatial functions with two complex components corresponding to two orthogonal linear polarizations. As a result we derive a Jones matrix that describes the polarization output in terms of two vectorial functions defining respectively the structured polarization input and the generalized polarization impulse response. We apply the method to show and analyze an experiment in which a regular scalar diffraction grating is converted into equivalent polarization diffraction gratings by means of an appropriate polarization filtering. The technique is further demonstrated to generate arbitrary structured polarizations. Excellent experimental results are presented.

©2011 Optical Society of America

OCIS codes: (260.5430) Polarization; (350. 2770) Gratings; (230.6120) Spatial light modulators; (070.2615) Frequency filtering.

References and links

1. J. A. Davis, D. E. McNamara, D. M. Cottrell, and T. Sonehara, "Two-dimensional polarization encoding with a phase-only liquid-crystal spatial light modulator," *Appl. Opt.* **39**(10), 1549–1554 (2000).
2. Z. Bomzon, V. Kleiner, and E. Hasman, "Formation of radially and azimuthally polarized light using space-variant subwavelength metal stripe gratings," *Appl. Phys. Lett.* **79**(11), 1587–1589 (2001).
3. V. Ramírez-Sánchez, and G. Piquero, "Global beam shaping with nonuniformly polarized beams using amplitude transmittances," *Opt. Pura Apl.* **40**, 87–93 (2007).
4. A. Volke, and G. Heine, "Bringing order into light with structured polarizers," *Photonik Int.* **2**, 6–9 (2008).
5. M. Stalder, and M. Schadt, "Linearly polarized light with axial symmetry generated by liquid-crystal polarization converters," *Opt. Lett.* **21**(23), 1948–1950 (1996).
6. R. Dorn, S. Quabis, and G. Leuchs, "Sharper focus for a radially polarized light beam," *Phys. Rev. Lett.* **91**(23), 233901 (2003).
7. Q. Zhan, "Cylindrical vector beams: from mathematical concepts to applications," *Adv. Opt. Photon.* **1**(1), 1–57 (2009).
8. J. A. Davis, G. H. Evans, and I. Moreno, "Polarization-multiplexed diffractive optical elements with liquid-crystal displays," *Appl. Opt.* **44**(19), 4049–4052 (2005).
9. M. Fratz, D. M. Giel, and P. Fischer, "Digital polarization holograms with defined magnitude and orientation of each pixel's birefringence," *Opt. Lett.* **34**(8), 1270–1272 (2009).
10. G. Cincotti, "Polarization gratings: Design and applications," *IEEE J. Quantum Electron.* **39**(12), 1645–1652 (2003).
11. F. Gori, "Measuring Stokes parameters by means of a polarization grating," *Opt. Lett.* **24**(9), 584–586 (1999).
12. J. A. Davis, J. Adachi, C. R. Fernández-Pousa, and I. Moreno, "Polarization beam splitters using polarization diffraction gratings," *Opt. Lett.* **26**(9), 587–589 (2001).
13. C. Oh, and M. J. Escuti, "Achromatic diffraction from polarization gratings with high efficiency," *Opt. Lett.* **33**(20), 2287–2289 (2008).
14. J. L. Martínez, I. Moreno, and F. Mateos, "Hiding binary optical data with orthogonal circular polarizations," *Opt. Eng.* **47**(3), 030504 (2008).
15. B. Javidi, and T. Nomura, "Polarization encoding for optical security systems," *Opt. Eng.* **39**(9), 2439–2443 (2000).
16. H.-Y. Tu, C.-J. Cheng, and M.-L. Chen, "Optical image encryption based on polarization encoding by liquid crystal spatial light modulators," *J. Opt. A, Pure Appl. Opt.* **6**(6), 524–528 (2004).
17. M. A. A. Neil, F. Massoumian, R. Juškaitis, and T. Wilson, "Method for the generation of arbitrary complex vector wave fronts," *Opt. Lett.* **27**(21), 1929–1931 (2002).

18. K. C. Toussaint, Jr., S. Park, J. E. Jureller, and N. F. Scherer, "Generation of optical vector beams with a diffractive optical element interferometer," *Opt. Lett.* **30**(21), 2846–2848 (2005).
 19. X.-L. Wang, J. Ding, W.-J. Ni, C.-S. Guo, and H.-T. Wang, "Generation of arbitrary vector beams with a spatial light modulator and a common path interferometric arrangement," *Opt. Lett.* **32**(24), 3549–3551 (2007).
 20. C. Maurer, A. Jesacher, S. Fürhapter, S. Bernet, and M. Ritsch-Marte, "Tailoring of arbitrary optical vector beams," *N. J. Phys.* **9**(3), 78 (2007).
 21. F. Gori, "Matrix treatment for partially polarized, partially coherent beams," *Opt. Lett.* **23**(4), 241–243 (1998).
 22. F. Gori, M. Santarsiero, R. Borghi, and G. Piquero, "Use of the van Cittert-Zernike theorem for partially polarized sources," *Opt. Lett.* **25**(17), 1291–1293 (2000).
 23. E. Wolf, *Introduction to the Theory of Coherence and Polarization of Light* (Cambridge University Press, Cambridge 2007).
 24. I. Moreno, M. J. Yzuel, J. Campos, and A. Vargas, "Jones matrix treatment for polarization Fourier optics," *J. Mod. Opt.* **51**(14), 2031–2038 (2004).
 25. I. Moreno, C. Iemmi, J. Campos, and M. J. Yzuel, "Binary polarization pupil filter: Theoretical analysis and experimental realization with a liquid crystal display," *Opt. Commun.* **264**(1), 63–69 (2006).
 26. I. Moreno, C. Iemmi, J. Campos, M. J. Yzuel, and A. Vargas, "Polarization vortices generation by diffraction from a four quadrant polarization mask," *Opt. Commun.* **276**(2), 222–230 (2007).
 27. A. Martínez-García, I. Moreno, M. M. Sánchez-López, and P. García-Martínez, "Operational modes of a ferroelectric LCoS modulator for displaying binary polarization, amplitude, and phase diffraction gratings," *Appl. Opt.* **48**(15), 2903–2914 (2009).
 28. I. Moreno, J. Campos, C. Gorecki, and M. J. Yzuel, "Effects of amplitude and phase mismatching errors in the generation of a kinoform for pattern recognition," *Jpn. J. Appl. Phys.* **34**, 6423–6432 (1995).
-

1. Introduction

The generation of two dimensional polarization distributions has received great attention in the last years, and different methods to generate light beams with structured polarization have been theoretically proposed and experimentally probed, including the use of liquid crystal spatial light modulators [1], sub-wavelength gratings [2], polarization interferometric setups [3], or linear polarizers with spatial variation [4]. Such polarization encodings have been successfully exploited in a variety of applications ranging from the formation of radially or azimuthally polarized beams [5], for producing sharper focusing [6,7], the formation of polarization sensitive computer generated holograms [8,9], or the realization of the so called polarization diffraction gratings [10], gratings with a periodic variation of the polarization component, with applications in polarimetry [11,12] or in the design of high efficient gratings [13]. Polarization encoding has also been used for security systems either to hide [14] or to encrypt information [15,16].

Recently, some other approaches to produce polarization maps have been proposed for different applications [17–20], which employ optical setups that can be considered as different variations of the classical optical Fourier processor. For instance, in Ref [17], a Wollaston prism was employed to create linear phases with opposite sign for two orthogonal polarizations, in order to illuminate a ferroelectric liquid crystal modulator that displays a binary phase pattern. The proper adjustment of the phase displayed by the modulator permits to create a proper polarization structure around a diffraction order in Fourier plane, which can be filtered to produce at the final output plane the desired polarization map. In Ref [18], radially and azimuthally polarized vector beams were generated by means of a diffractive optical element (DOE) interferometer, where the two first diffracted orders are directed to two half-wave plates with different orientation. A second identical DOE recombines the two transmitted beams to create the desired polarization distribution. Similar techniques were employed to create more complicated polarized beams in Refs [19]. and [20], where different types of polarization filtering were applied to two modulated beams that were then recombined. All these works treat the polarization transformations step by step, usually employing Jones vectors to DESCRIBE the states in each plane (input mask, diffraction Fourier plane, recombination output plane).

Recently, the study of the propagation of light beams with arbitrary general polarization structure has been analyzed by means of the beam coherence polarization (BCP) matrix [21–23]. This method permits to derive the complex vectorial diffraction pattern generated by a diffractive mask with spatial polarization and coherence dependence. In Ref [24], we presented a simplified approach that combines the usual Jones matrix formalism and

the Fourier transform to analyze in a very compact polarization diffractive elements with spatial variations larger than the wavelength (so the scalar diffraction can be applied). The method applies only to fully polarized and fully coherent illumination, but this is the usual case employed in systems like in Refs [16–20]. The method in [24] allows describing the whole polarization transformation from the input to the Fourier diffraction plane in a single step using the usual Jones matrices. We applied this approach to analyze polarization pupil filters [25], polarization quadrant masks [26], or polarization diffraction gratings [27]. The goal of this paper is to extend these previous works to analyze polarization optical processors as described above by means of the combined Jones matrix – Fourier transform formalism, and show how it can be applied to easily analyze the output polarization map. For that purpose, we develop a generalization of optical processing systems to polarization (vectorial) systems, and present some examples of its application to generate polarization maps.

The paper is organized as follows: in section 2 we introduce the Jones matrix – Fourier transform formalism, and extend it to the optical processor. In section 3 we present how it can be applied to generate polarization diffraction gratings from a regular scalar diffraction grating filtered in the Fourier plane by means of polarization elements. Finally in section 4 we extend this processor to create arbitrary maps of linear polarizations with variable orientation, controlled from the phase introduced by a phase-only spatial light modulator located at the input plane. In all cases, the theoretical analysis based on the combined Jones matrix – Fourier transform formalism is accompanied with experimental demonstration of the generated polarization patterns.

2. Jones matrix analysis of an optical Fourier polarization processor

Let us consider a generalized optical Fourier processor as sketched in Fig. 1, where both the input plane and the Fourier filter plane are spatially dependant polarization masks. For simplicity we consider the classical $4f$ configuration with two convergent lenses with equal focal length. The input polarization mask can be described by a Jones matrix which depends on the spatial coordinates (x,y) as

$$f(x, y) = \begin{pmatrix} f_{xx}(x, y) & f_{xy}(x, y) \\ f_{yx}(x, y) & f_{yy}(x, y) \end{pmatrix}. \quad (1)$$

Following Ref [21], the propagation from the input to the Fourier transform plane can be described by a Fourier-Jones matrix given by

$$F(u, v) = \begin{pmatrix} F_{xx}(u, v) & F_{xy}(u, v) \\ F_{yx}(u, v) & F_{yy}(u, v) \end{pmatrix}, \quad (2)$$

where $F_{ij}(u, v) = \text{FT}\{f_{ij}(x, y)\}$, being **FT** the Fourier transform operation and (u,v) denoting the spatial frequencies, which are related to the spatial coordinates in the filter plane as

$$u = \frac{x}{\lambda f}, \quad v = \frac{y}{\lambda f}, \quad (3)$$

being λ the wavelength of the light and f the focal length of the lens.

The polarization mask introduced in the Fourier plane (the generalized polarization transfer function) is also characterized by a polarization transmission described by a spatially variant Jones matrix defined as

$$H(u, v) = \begin{pmatrix} H_{xx}(u, v) & H_{xy}(u, v) \\ H_{yx}(u, v) & H_{yy}(u, v) \end{pmatrix}. \quad (4)$$

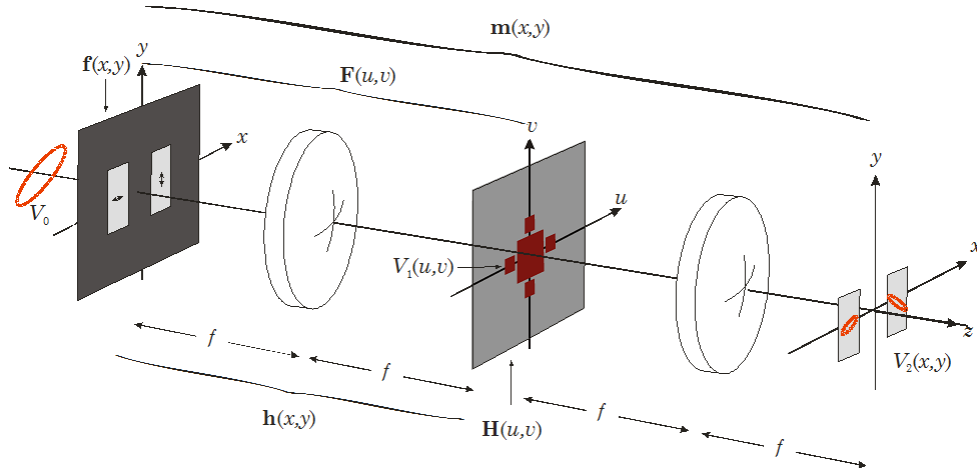


Fig. 1. Scheme of the optical Fourier transform polarization processor.

The Jones matrix $\mathbf{h}(x,y)$ defined as

$$\mathbf{h}(x,y) = \begin{pmatrix} h_{xx}(x,y) & h_{xy}(x,y) \\ h_{yx}(x,y) & h_{yy}(x,y) \end{pmatrix}, \quad (5)$$

where

$$h_{ij}(x,y) = \text{FT}^{-1} \{ H_{ij}(u,v) \}, \quad (6)$$

is obtained by inverse Fourier transforming each element of the Jones matrix in Eq. (4), and can be interpreted as the vectorial (polarization) generalization of the scalar impulse response of the classical scalar optical processor.

The passage of light through the input mask, propagation to the Fourier plane, and passage through the polarization filter, is given by the usual Jones matrix product, i.e.:

$$\begin{aligned} \mathbf{H}(u,v) \mathbf{F}(u,v) &= \begin{pmatrix} H_{xx}(u,v) & H_{xy}(u,v) \\ H_{yx}(u,v) & H_{yy}(u,v) \end{pmatrix} \begin{pmatrix} F_{xx}(u,v) & F_{xy}(u,v) \\ F_{yx}(u,v) & F_{yy}(u,v) \end{pmatrix} = \\ &= \begin{pmatrix} H_{xx}F_{xx} + H_{xy}F_{yx} & H_{xx}F_{xy} + H_{xy}F_{yy} \\ H_{yx}F_{xx} + H_{yy}F_{yx} & H_{yx}F_{xy} + H_{yy}F_{yy} \end{pmatrix}, \end{aligned} \quad (7)$$

where we omitted (u,v) dependence for clarity. The propagation to the final output plane implies another Fourier transformation and, therefore, the whole transformation from the input to the output plane can be described by a Jones matrix $\mathbf{m}(x,y)$ obtained by Fourier transforming each element of the matrix in Eq. (7), i.e.:

$$\mathbf{m}(x,y) = \begin{pmatrix} h_{xx} \otimes f_{xx} + h_{xy} \otimes f_{yx} & h_{xx} \otimes f_{xy} + h_{xy} \otimes f_{yy} \\ h_{yx} \otimes f_{xx} + h_{yy} \otimes f_{yx} & h_{yx} \otimes f_{xy} + h_{yy} \otimes f_{yy} \end{pmatrix}, \quad (8)$$

where the symbol \otimes denotes the convolution operation, and where, for clarity, we omitted the (x,y) dependence of the h_{ij} and f_{ij} functions. This equation can be written in a compact way as

$$\mathbf{m}(x,y) = \mathbf{f}(x,y) \bar{\otimes} \mathbf{h}(x,y), \quad (9)$$

where the symbol $\bar{\otimes}$ denotes a generalized convolution between the two Jones matrices as defined by Eq. (8).

The interest of the proposed formalism comes from the direct application of the Jones matrix calculus to obtain the output polarization maps. If the generalized polarization processor is illuminated with a polarized plane wave with a polarization state described by the Jones vector V_0 , the polarization maps $V_1(u,v)$ just before the polarization filter at the Fourier plane, and $V_2(x,y)$ at the final output plane, are given respectively by

$$V_1(u,v) = F(u,v) \cdot V_0, \quad V_2(x,y) = m(x,y) \cdot V_0. \quad (10)$$

Next we will present two examples on the application of this formalism.

3. Polarization gratings generated from scalar diffraction gratings

As a first example we present a very simple method to generate polarization diffraction gratings from a regular scalar diffraction grating through Fourier polarization filtering. For simplicity, we consider a diffraction grating that generates only the ± 1 diffraction orders. The Jones matrix in Eq. (1) describing the input polarization mask can be written in this case as $\mathbf{f}(x,y) = \cos(\pi ax) \cdot \mathbf{1}$ where $\mathbf{1}$ denotes the 2×2 identity matrix, being $p=2/a$ the period of the grating. The complex amplitude generated at the Fourier plane is given by

$$\mathbf{F}(u,v) = \frac{1}{2} (\delta(u-a,v) + \delta(u+a,v)) \cdot \mathbf{1}. \quad (11)$$

The state of polarization in the two generated diffraction orders is the same as that of the incoming beam. The realization of the spatially periodic polarization structure that characterizes polarization diffraction gratings is obtained by modifying the polarization of each of the two diffraction orders in a different manner. For instance, let us consider two quarter-wave plates (QWP) located on each diffraction order, but oriented at 0 and 90° respectively (i.e., one QWP has the fast axis horizontal, while the second one has the fast axis vertical). The Jones matrix $\mathbf{H}(u,v)$ in Eq. (4) describing this simple Fourier filter is given by

$$\begin{aligned} \mathbf{H}(u,v) &= P(u-a,v) \mathbf{QWP}_{\theta=90^\circ} + P(u+a,v) \mathbf{QWP}_{\theta=0^\circ} = \\ &= P(u,v) \otimes \left\{ \delta(u-a,v) \begin{pmatrix} +i & 0 \\ 0 & 1 \end{pmatrix} + \delta(u+a,v) \begin{pmatrix} 1 & 0 \\ 0 & +i \end{pmatrix} \right\} = \\ &= P(u,v) \otimes \begin{pmatrix} i\delta(u-a,v) + \delta(u+a,v) & 0 \\ 0 & \delta(u-a,v) + i\delta(u+a,v) \end{pmatrix}, \end{aligned} \quad (12)$$

where \mathbf{QWP}_θ denotes the Jones matrix for a quarter wave plate oriented at angle θ , i.e.:

$$\mathbf{QWP}_\theta = \mathbf{R}(-\theta) \cdot \begin{pmatrix} 1 & 0 \\ 0 & +i \end{pmatrix} \cdot \mathbf{R}(+\theta), \quad (13)$$

being $\mathbf{R}(\theta)$ the 2×2 rotation matrix. $P(u,v)$ in Eq. (12) denotes a binary amplitude function describing the physical aperture of each QWP, which we assume identical and having a size smaller than $a\lambda f$. The generalized Jones matrix impulse response of this simple polarization Fourier filter is given by inverse Fourier transforming the elements in Eq. (12), leading to

$$\begin{aligned} \mathbf{h}(x,y) &= p(x,y) \cdot \begin{pmatrix} ie^{+i\pi ax} + e^{-i\pi ax} & 0 \\ 0 & e^{+i\pi ax} + ie^{-i\pi ax} \end{pmatrix} = \\ &= p(x,y) \cdot 2e^{i\frac{\pi}{4}} \begin{pmatrix} \cos(\pi ax + \frac{\pi}{4}) & 0 \\ 0 & \sin(\pi ax + \frac{\pi}{4}) \end{pmatrix}, \end{aligned} \quad (14)$$

where $p(x,y) = \mathbf{F}\mathbf{T}^{-1}\{P(u,v)\}$, and where we employed the trigonometrical relations $\cos(x) - \sin(x) = \sqrt{2} \cos(x + \frac{\pi}{4})$ and $\cos(x) + \sin(x) = \sqrt{2} \sin(x + \frac{\pi}{4})$. Note that this polarization impulse response is similar to the generalized two aperture polarization interference that was analyzed in Ref [24].

Since the diffraction orders are located on the center of the corresponding QWP, the product $\mathbf{H}(u,v)\mathbf{F}(u,v)$ in Eq. (7) is simplified to:

$$\mathbf{H}(u,v)\mathbf{F}(u,v) = \frac{1}{2} \begin{pmatrix} i\delta(u-a,v) + \delta(u+a,v) & 0 \\ 0 & \delta(u-a,v) + i\delta(u+a,v) \end{pmatrix}. \quad (15)$$

Either inverse Fourier transforming this Jones matrix or equivalently calculating the result in Eq. (8), the whole polarization Fourier processor is described by the Jones matrix $\mathbf{m}(x,y)$:

$$\mathbf{m}(x,y) = e^{i\frac{\pi}{4}} \begin{pmatrix} \cos(\pi ax + \frac{\pi}{4}) & 0 \\ 0 & \sin(\pi ax + \frac{\pi}{4}) \end{pmatrix}. \quad (16)$$

Let us now assume that the polarization Fourier processor is illuminated with linearly polarized light oriented at 45° , so the input Jones vector is given by

$$V_0 = \frac{1}{\sqrt{2}} \begin{pmatrix} 1 \\ 1 \end{pmatrix}. \quad (17)$$

The vectorial (polarization) distribution at the output plane of the optical processor is given by

$$V_2(x,y) = \mathbf{m}(x,y) \cdot V_0 = \frac{e^{i\frac{\pi}{4}}}{\sqrt{2}} \begin{pmatrix} \cos(\pi ax + \frac{\pi}{4}) \\ \sin(\pi ax + \frac{\pi}{4}) \end{pmatrix}. \quad (18)$$

The result is a one dimensional periodic distribution of linear polarization states, where the orientation θ of the linear polarization varies as $\theta(x) = \pi ax + \pi/4$, i.e., with the same period $2/a$ as the grating in the input plane. This polarization distribution is basically equivalent to the one generated with the polarization diffraction grating proposed by Gori in Ref [11]. Figure 2(a) shows a scheme of this proposed polarization optical Fourier processor and the output when it is illuminated with linear polarization at 45° .

Another interesting case is obtained when the same polarization Fourier processor is illuminated with right handed circularly polarized light (Fig. 2(b)). In this case V_0 is

$$V_0 = \frac{1}{\sqrt{2}} \begin{pmatrix} 1 \\ +i \end{pmatrix}, \quad (19)$$

and the vectorial (polarization) distribution at the output plane of the optical processor is now given by

$$V_2(x,y) = \mathbf{m}(x,y) \cdot V_0 = \frac{e^{i\frac{\pi}{4}}}{\sqrt{2}} \begin{pmatrix} \cos(\pi ax + \frac{\pi}{4}) \\ +i \sin(\pi ax + \frac{\pi}{4}) \end{pmatrix}. \quad (20)$$

Now the result is again a one dimensional periodic distribution of polarization states along the x -direction, with the same period $2/a$, but now the polarization states are always elliptical, with ellipses centered on the x - y axes (i.e., the azimuth is fixed at 0 - 90°), being now the ellipticity the parameter that is periodically changed.

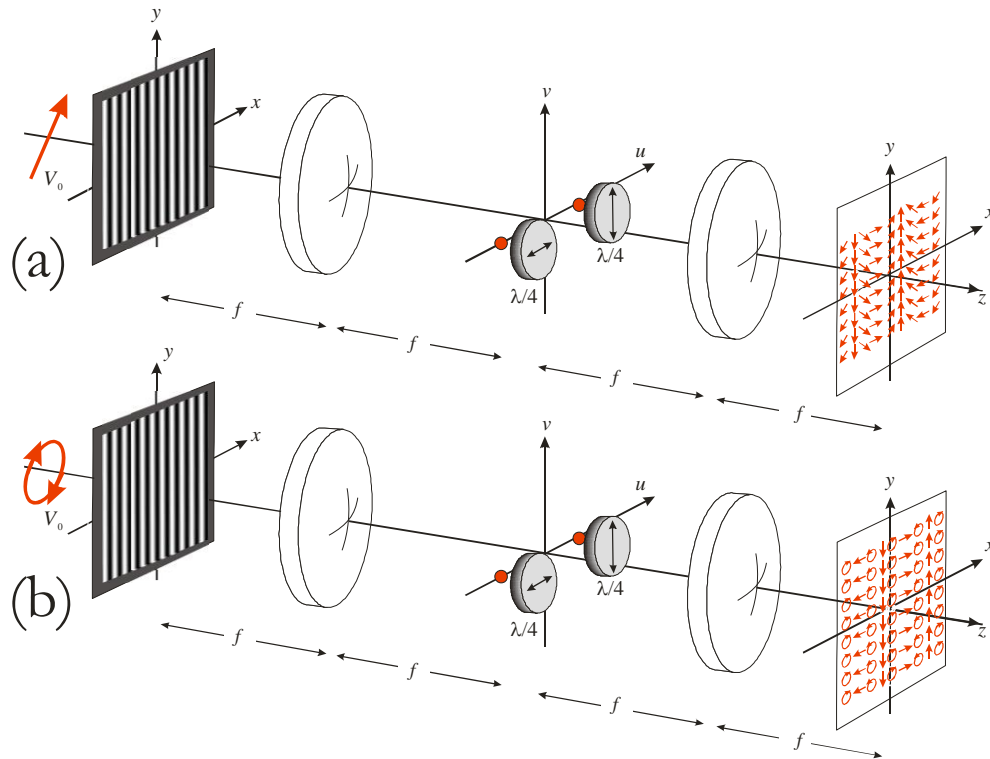


Fig. 2. Scheme of the optical Fourier transform polarization processor to generate polarization diffraction gratings. (a) Illumination with linearly polarized light oriented at 45° produces an output with a periodic map of linear polarizations with variable orientation. (b) Illumination with circularly polarized light produces an output with a periodic map of elliptical polarizations with fixed azimuth and variable ellipticity.

We have experimentally built such a polarization Fourier processor. We employed regular phase grating at the input plane, and two QWPs with small aperture at the Fourier plane. We blocked all but the ± 1 generated diffraction orders, and placed two QWPs on their location with the adequate orientation. We used a CCD camera with a microscope objective to visualize the final output plane. In order to visualize the polarization nature of the periodic distribution in the output plane, we placed a linear polarizer analyzer just before the objective.

Figure 3 shows the experimental result obtained at the final output plane. Figure 3(a) shows the case when the processor is illuminated with linear polarization oriented at 45° , while the analyzer is oriented horizontal (at 0°). Vertical interference fringes are visible. As we change the orientation (θ) of the analyzer the fringes shift laterally. Null fringes are located always at the position where the output linear polarization is oriented crossed to the analyzer. We generated a composite image (Fig. 3(b)), where the same narrow horizontal band is selected in images captured for each value of θ . It shows how the fringes are shifted laterally, but the contrast is maintained maximum, denoting the expected periodic sequence of linear polarizations as derived from Eq. (18). The related video shows the fringe displacement as we rotate the analyzer. The output changes when the polarization illuminating the input plane in the processor is a right handed circular polarized plane wave (Figs. 3(c) and 3(d)). In this case the rotation of the analyzer results in a variation of the contrast of the fringes, without lateral shift. Figure 3(c) shows the captured image when the analyzer is oriented at 45° . In this situation, the output periodic polarization map results in a uniform image, since the entire polarization states project to the analyzer with half the incoming intensity. On the contrary, when the analyzer is oriented either horizontal (0°) or vertical (90°), the contrast of the fringes becomes maximal (although a contrast inversion is produced between these two

cases). All these results correspond to the behavior expected from the periodic Jones vector pattern in Eq. (20).

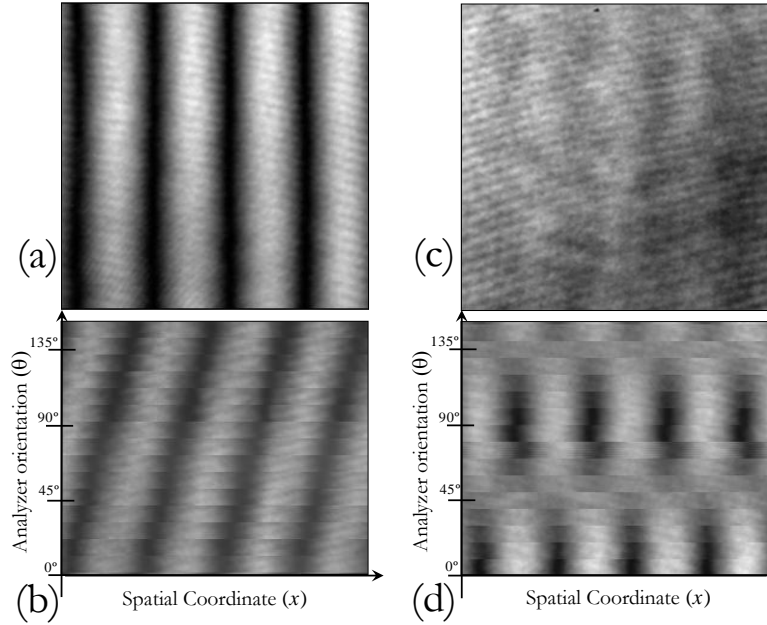


Fig. 3. Experimental interference fringes at the output plane for (a) (Media 1) Illumination with linearly polarized light oriented at 45° and analyzer at 0° . (c) Illumination with right handed circularly polarized light and analyzer at 45° . (b)-(d) Evolution of the fringe pattern as a function of the orientation (θ) of the final analyzer corresponding to illumination with: (b) (Media 2) Linear polarization at 45° and (d) Circular right polarization.

4. Generation of arbitrary structured linear polarization maps

Next, as a second useful example, we extend the previous method to generate arbitrary maps of linear polarizations. For that purpose we follow a similar scheme as in Refs [19,20], but we use a spatial light modulator at the input plane operating in a binary-phase mode, and a simple polarization filtering similar to that in the previous section. The aim here is to generate an arbitrary spatial distribution of linear polarized states, which therefore can be described in the form of an output Jones vector

$$V_2(x, y) = \begin{pmatrix} \cos(\alpha(x, y)) \\ \sin(\alpha(x, y)) \end{pmatrix}, \quad (21)$$

where $\alpha(x, y)$ is the orientation of the linear polarization at the location (x, y) . In order to produce such distribution, we encode the angle α in the form of the phase introduced by a phase-only spatial light modulator located on the input plane as:

$$f(x, y) = \exp\{i[\alpha(x, y) + \pi ax]\}. \quad (22)$$

This phase-only function generates, in the Fourier plane, the function $A(u, v) = \mathbf{FT}\{\exp[i\alpha(x, y)]\}$, centered at the spatial frequency $u=a$. If the phase-only function in Eq. (22) is binarized to phase values 0 and π , the resulting function, $f_{\text{BIN}}(x, y) = \text{BIN}\{f(x, y)\}$, can be directly implemented in a binary phase modulator. Since this is a scalar phase function, the input mask does not affect the polarization and it can be written as

$$f(x, y) = f_{\text{BIN}}(x, y) \cdot 1. \quad (23)$$

Thus, it generates a diffraction pattern whose main contributions are the direct expected Fourier transform function $A(u,v)$ centered at the expected location $u=a$, and its complex conjugated version located at the location $u=-a$ (each one carrying $(2/\pi)^2=40.3\%$ of the total energy in the Fourier plane) [28]. Ignoring this amplitude factor, it can be expressed as:

$$\mathbf{F}(u,v) \cong \{ A(u-a,v) + A^*(-u-a,-v) \} \cdot \mathbf{1}. \quad (24)$$

The key point to produce the polarization map is to convert each of these terms into circularly polarized beams, but with opposite helicity. Therefore, we could use a polarization filter similar to the one in the previous section. However, as we describe later, it is necessary to make the two beams collinear. To do that, we employ a mirror and a beam splitter in a system as drawn in Fig. 4. We employ a polarization beam splitter (PBS), and a QWP located behind it. The PBS acts as a linear polarizer for each ± 1 diffraction orders, but with orthogonally oriented transmission axis. It acts as a vertical linear polarizer for the $+1$ diffraction order, and as a horizontal linear polarizer for the -1 diffraction order. The QWP is oriented at $+45^\circ$, so the two beams become circularly polarized after traversing it, but with opposite helicity.

We assume that the spatial bandwidth of the function $A(u,v)$ fits within the aperture $P(u,v)$ of the QWP's. Therefore, the product $\mathbf{H}(u,v)\mathbf{F}(u,v)$ in Eq. (7) can be now written as:

$$\mathbf{H}(u,v)\mathbf{F}(u,v) = A(u-a,v)\mathbf{QWP}_{45}\mathbf{P}_0 + A^*(-u-a,-v)\mathbf{QWP}_{45}\mathbf{P}_{90}. \quad (25)$$

where \mathbf{P}_0 and \mathbf{P}_{90} denote the Jones matrices for linear polarizers oriented at 0° and 90° , i.e.:

$$\mathbf{P}_0 = \begin{pmatrix} 1 & 0 \\ 0 & 0 \end{pmatrix}, \quad \mathbf{P}_{90} = \begin{pmatrix} 0 & 0 \\ 0 & 1 \end{pmatrix}, \quad (26)$$

and where \mathbf{QWP}_{45} adopts the form:

$$\mathbf{QWP}_{45} = \mathbf{R}(-45^\circ) \cdot \begin{pmatrix} 1 & 0 \\ 0 & +i \end{pmatrix} \cdot \mathbf{R}(+45^\circ) = \frac{e^{i\frac{\pi}{4}}}{\sqrt{2}} \begin{pmatrix} 1 & -i \\ -i & 1 \end{pmatrix}. \quad (27)$$

The explicit calculation of Eq. (25) leads to

$$\mathbf{H}(u,v)\mathbf{F}(u,v) = \frac{e^{i\frac{\pi}{4}}}{\sqrt{2}} \begin{pmatrix} A(u-a,v) & -iA^*(-u-a,-v) \\ -iA(u-a,-v) & A^*(-u-a,-v) \end{pmatrix}. \quad (28)$$

Therefore, the Jones matrix $\mathbf{m}(x,y)$ describing the complete polarization processor is obtained by inverse Fourier transforming each component in the above matrix, i.e.,

$$\mathbf{m}(x,y) = \frac{e^{i\frac{\pi}{4}}}{\sqrt{2}} \begin{pmatrix} e^{i[\alpha(x,y)+\pi ax]} & -ie^{-i[\alpha(x,y)+\pi ax]} \\ -ie^{i[\alpha(x,y)+\pi ax]} & e^{-i[\alpha(x,y)+\pi ax]} \end{pmatrix}. \quad (29)$$

Let us assume that the input polarization to the optical processor is linearly polarized oriented at 45° . Then the final polarization distribution can be obtained in a direct way from the product $V_2(x,y) = \mathbf{m}(x,y) \cdot V_0$, where $\mathbf{m}(x,y)$ and V_0 are given by Eqs. (29) and (17) respectively. The result is

$$V_2(x,y) = \begin{pmatrix} \cos \left\{ \alpha(x,y) + \pi ax + \frac{\pi}{4} \right\} \\ \sin \left\{ \alpha(x,y) + \pi ax + \frac{\pi}{4} \right\} \end{pmatrix}, \quad (30)$$

where the same trigonometric relations used to derive Eq. (14) are employed here. Note that this result in Eq. (30) basically provides the desired result in Eq. (21), except for the linear term πax and the $\pi/4$ phase factor within the sine and cosine functions. While the $\pi/4$ phase factor implies this additional rotation, which can be simply compensated in the design of the function α , the linear phase terms in Eq. (30) contribute to modify the orientation of the

polarization states in the final plane by adding a periodic variation. Therefore, it is necessary to eliminate these linear phases. The system in Ref [19], is a diffraction interferometer, where a diffraction grating was introduced on the final plane in order to eliminate these linear phase terms. Here we use an alternative setup as shown in Fig. 4, where the two beams coming from the two diffraction orders at the Fourier plane are made collinear with the help of a mirror (M) and the polarization beam splitter (PBS). Once the two beams are collinear, they are Fourier transformed by the second converging lens and the SLM is imaged onto the CCD camera (note that the final Fourier transformation in the experiment is a direct transform, as opposite to the inverse transform considered to derive Eq. (29), but the result is equivalent except for an inversion).

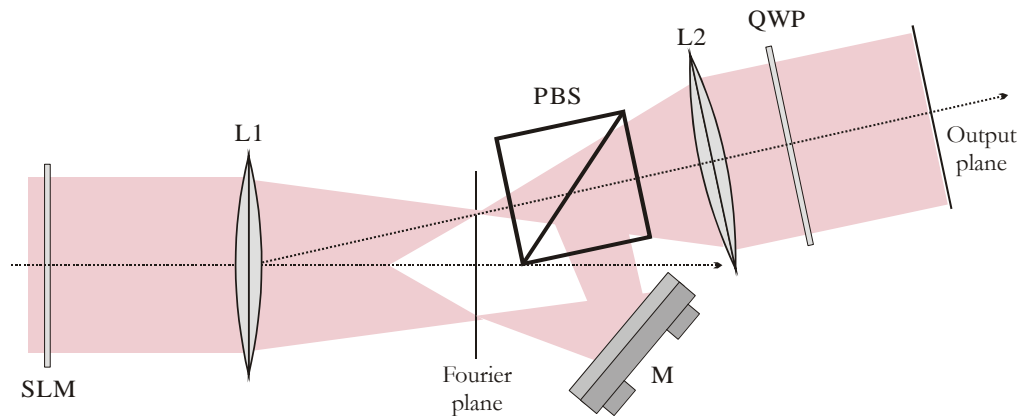


Fig. 4. Experimental arrangement for the production of arbitrary polarization map by means of a polarization Fourier processor. PBS is a polarizing beam splitter, QWP is a quarter wave plate oriented at 45° , L1 and L2 are converging lenses, and M a mirror.

As input binary phase SLM we employ a liquid crystal display sandwiched between two linear polarizers. Thus, this is a polarization device which must be described with a corresponding Jones matrix. However, if the polarization emerging from the SLM is split with equal power by the PBS, the simpler above results are reproduced. Figure 5 shows the experimental results obtained with this setup. Figure 5(a) shows a simple distribution of linear polarizations that we want to generate. This is encoded by properly selecting the angle α in the input image. Figure 5(b) shows the CCD capture of the output plane of the optical processor, when no final analyzer is placed. In this situation the different orientations of the linear polarization in each region is not visible. In order to visualize them we placed the analyzer just before the output plane, and captured images when rotating it. Then, the area of the final image with a linear polarization crossed to the transmission axis of the polarizer appears as dark. When the analyzer is oriented horizontal (Fig. 5(c)), the circle appears bright and the background appears dark. The situation is reversed when the analyzer is oriented vertical (Fig. 5(e)). Also note that the circle is confused with the background when the analyzer is oriented at 45° or 135° (Figs. 5(d) and 5(f)), since the horizontal and vertical linear polarizations are transmitted with equal energy through the analyzer.

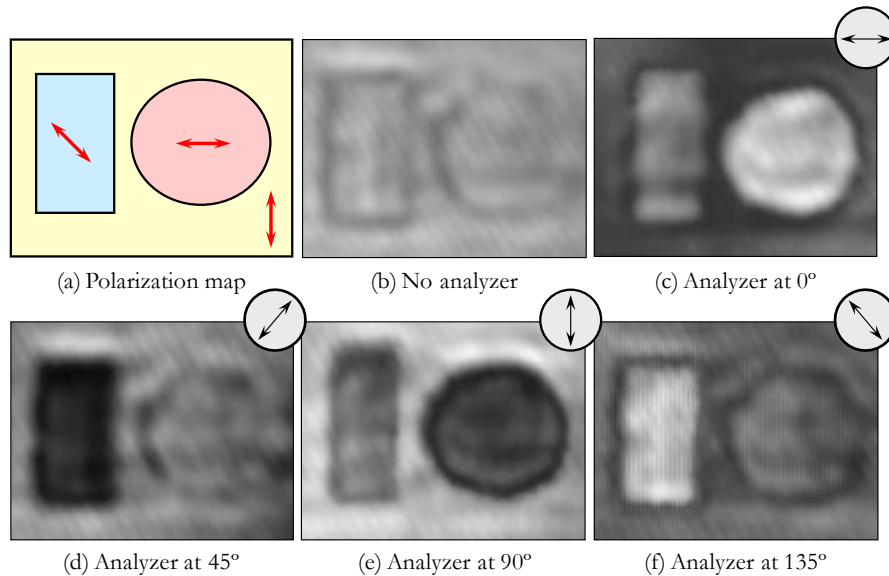


Fig. 5. (a) Desired polarization map. Experimental results obtained at the output plane for (b) absence of the analyzer and analyzer oriented at (c) 0°, (d) 45°, (e) 90° and (f) 135°.

5. Conclusions

In summary, we presented a Jones matrix based formalism to analyze an optical Fourier processor. This formalism extends our previously reported method to analyze a polarization Fourier transform diffractometer [24], and it is revealed here as a useful tool to analyze optical Fourier processors where local changes in the polarization can occur either in the input plane, in the Fourier plane, or in both planes. We extend classical Fourier optics concepts to vectorial polarization functions, like for instance the Jones matrix $\mathbf{h}(x,y)$ which generalizes the impulse response of frequency Fourier filter. As a result of this whole Fourier analysis, we derive a spatial Jones matrix $\mathbf{m}(x,y)$ which describes the actuation of the complete polarization processor on the Jones vector V_0 describing the state of polarization launched to the processor in its input plane. The final polarization pattern in the output plane is described as the spatially dependent Jones vector $V_2(x,y)$ directly calculated applying the usual Jones calculus as $V_2(x,y) = \mathbf{m}(x,y) \cdot V_0$.

We have presented two examples of application of such a polarization optical Fourier processor. The goal of the first one is to convert a regular scalar diffraction grating at the input plane into a periodic one dimensional distribution of polarization states on the output plane (equivalent to a polarization diffraction grating). For that purpose two QWPs are introduced in the Fourier plane, with orthogonal orientations, and centered on the location on the ± 1 diffraction orders. We presented how the processor is capable to generate different periodic polarization distributions depending on the input polarization. This system therefore permits to reproduce a polarization diffraction grating from a regular grating, using very simple optical components.

As a second example, we extended the previous method to generate arbitrary maps of linear polarizations. A phase-only spatial light modulator is introduced in the input plane to generate phase maps, and a variation of the previous two QWPs polarization Fourier filter is introduced in the Fourier plane. As a result we demonstrated that arbitrary linear polarization distributions can be generated on the output plane, where the orientation of the linear polarization is controlled by the phase introduced at the input plane. The proposed polarization Fourier processor provides certain interesting advantages compared to other methods to generate arbitrary polarization patterns. For instance they can be used to generate patterns with arbitrary polarization states, without requirements of specially designed liquid

crystal displays, and employs simple optical elements, with very reduced cost compared to the equipment required to fabricate subwavelength grating patterns.

We have provided excellent experimental results for both presented examples, that probe the validity of the method and show its potentiality use in Fourier optics based polarization systems.

Acknowledgments

We acknowledge financial support from Ministerio de Ciencia e Innovación from Spain (ref. FIS2009-13955-C02-01 and -02). C. Iemmi gratefully acknowledges the support of the Universidad de Buenos Aires and CONICET (Argentina).